Article

Synthesis, Characterization and Antioxidant study of some Bivalent Metal complexes by N_2O_2 -donor crown macrocyclic ligand.

Noor S. Khdair , Sattar S. Ibrahim , Ali K. A. Al-Naseeri

Department of Chemistry, College of Science, University of Anbar, Ramadi, Iraq **E. mail:** cfw.ailkareem@uoanbar.edu.iq

E. mail: sc.sattar_salim1976@uoanbar.edu.iq

E. mail: noo22s3006@uoanbar.edu.iq

Abstract:

The synthesis prepared of 2,2"-[Ethane-1,2-dylbis(oxy)]dibenzaldehyde (N) is covered in the paper .The metal complexes of its were synthesized from the reaction of O-phenlyene diamine with the ligand . The N process of preparation was completed. underwent two phases in which the Na_2CO_3 intermediate in DMF reacted with two matching salicylic aldehydes. One 1,2-dibromoethane equivalent was then added. And then the ligand N was introduced, dissolved. Five novel compounds were prepared in DMF using a molar ratio of (0.5M:N:O - phenylene diamine). Physicochemical techniques (FTIR, electron spectroscopy, mass and ^{1}HNMR. ^{13}C-NMR susceptibility, and molar conductivity) were used to confirm the isolated compositional entity of the produced compounds. Based on characterization data, octahedral compounds exhibiting the chemical formula $[MLC1_2]$. Where (M = Co(ll), Ni(ll), Cu(ll), Zn (ll)and Cd(ll)) the antimicrobial activity of the title compounds (ligand and complexes) was tested as an antioxidant. The data obtained revealed that the mineral complexes became less active than Ligand.

Key Words: Complexes , Antioxidant, Macrocyclic, Ligand

INTRODUCTION

A cyclic molecule is referred to as a macrocyclic compound [1] when the ring has nine atoms or more, three of which have to be donors of electron pairs. Because they can selectively chelate Because they identify certain metal ions depending on the quantity, kind, and location of the donor , the ionic radius for their metallic centers, or the coordinating characteristic of counterions, macrocyclic Schiff compounds are crucial to macrocyclic chemistry [2-4]. Nonetheless, understanding the chemical of transition metal complexes can be very beneficial for fundamental research in fields like biology, catalysis, and magneto chemistry. [5-7]. Macrocyclic metal complexes exhibit intriguing biological properties such as antibiotic, antifungal, anticancer, and antiproliferative activities. [8- 11]. Furthermore, synthetic Because tetra deter macrocycles (N_2O_2) feature two nitrogen donor and two oxygen donor sites that are only permitted to stabilize peculiar oxidation states of coordinated metal ions, they have been considered as generally reliable models. All of the complexes were characterized using several physical and chemical techniques, such as FT-IR, UV-Vis, NMR, mass, and conductance measurements. were used to characterize all the complexes

Experimental Part.

The components used in this study came from commercial sources and were used without further purification. Using KBr discs, FTIR spectra were obtained between 4000 and 250 cm-1 on a the company Shimadzu Infrared Fourier Transform The spectrometer (FTIR-600). By using electromagnetic ionization (positive mode) and an Agilent mass spectrometer, ligand's mass spectrum was determined using Sciex ESI mass analysis. Using a Brucker-500 MHz a spectrum analyzer, ligand's ^1H and ^{13}C NMR spectra were captured in DMSO-d^6. Tetramethylsilane (TMS) was used as an internal standard to measure chemistry shifts. A Shimadzu UV-160 spectrometer was used to analyze the electronic spectra of substances in the 200–1000 nm region for 10^{-3} M solution in DMSO at ambient temperature. We used the electrothermal Stuart apparatus (model SMP40) to determine melting to determine melting points. C.H.N Dosimat Metrom Swiss was used for elemental analyses in order to determine the percentages of metals and chlorides. At 308 K, the magnetic moments were taken with a Sherwood Scientific apparatus. A digital conductivity meter, the Eutech Instrument Cyberscan con 510, was used to measure the molar conductance of complexes.

Preparation of 2,2′-(Ethane-1,2-diylbis(oxy))dibenzaldehyde (N)

The following procedure was used to Synthesis 2,2′-(Ethane-1,2-diylbis(oxy))dibenzaldehyde (N): After dissolving 1.22 g (10 mmol) of salicylic aldehyde in (10 ml) of DMF, 1.3 g (10 mmol) of sodium carbonate (Na_2Co_3) was added. After adding 1,2-di bromoethane (0.95 g , 5 mmol), the reaction was agitated for ten minutes at room temperature before being continued. To get brilliant brown crystals, The mixture was washed with ice water, filtered, and then re crystallized using ethanol. With a molecular mass of 270 g/mol and a melting temperature of 118–120°C, the final yield was 2.4 g (66%). bands at 1685 & 1666 cm-1 of ν(C=O) aldehyde, 1242 cm^{-1} of ν(C-O-C), , 1597 cm^{-1} for ν(C=C) were detected by FT-IR analysis (KBr). [12].

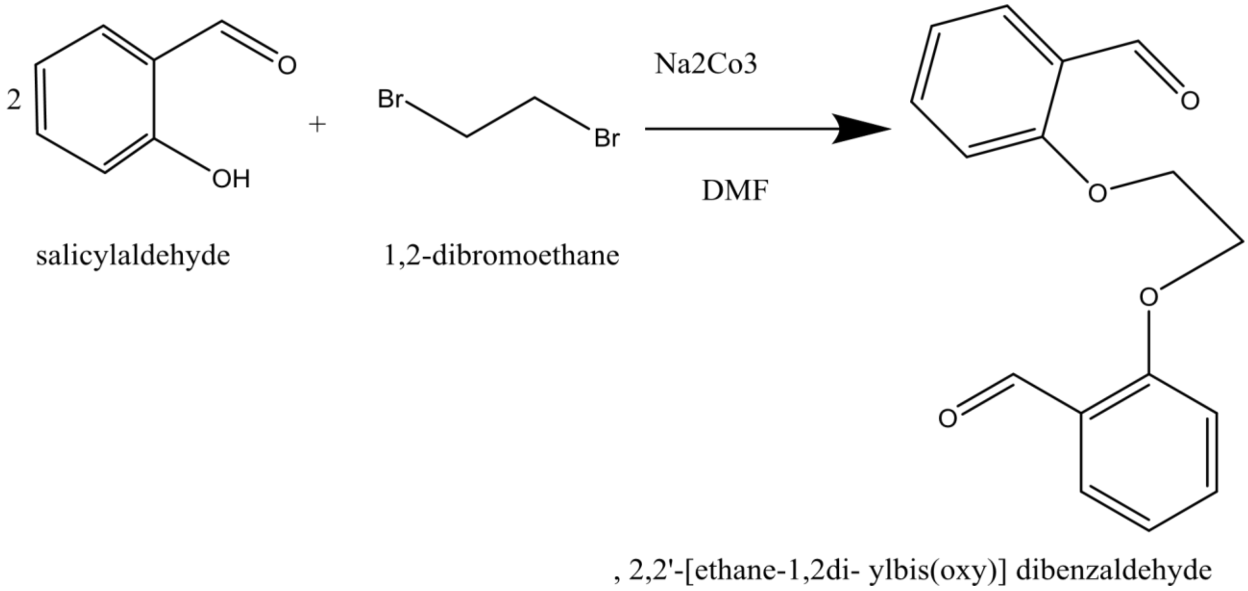

Scheme (1): The Preparation of 2,2′-(Ethane-1,2-diylbis(oxy))dibenzaldehyde (N).

Synthesis of metal complexes

The method used to make the complexes was to dissolve (1.06 g) of O-phenlyene diamine (0.01 mol) in (30 ml)of heated ethanol, then add the metal (II) salt(Co‹Ni‹Cu‹Zn and Cd) (0.005 mol) to the mixture. (10 ml) of ethanol. After 30 minutes of reflex, the solution for (N), which is (2.7g. 0.01 mol) was progressively added to (30 ml) of DMF. After four hours of reflex, the material was dumped into a glass container and allowed to sit for a time. It was then filtered and given a hot ethanol wash after that [13].

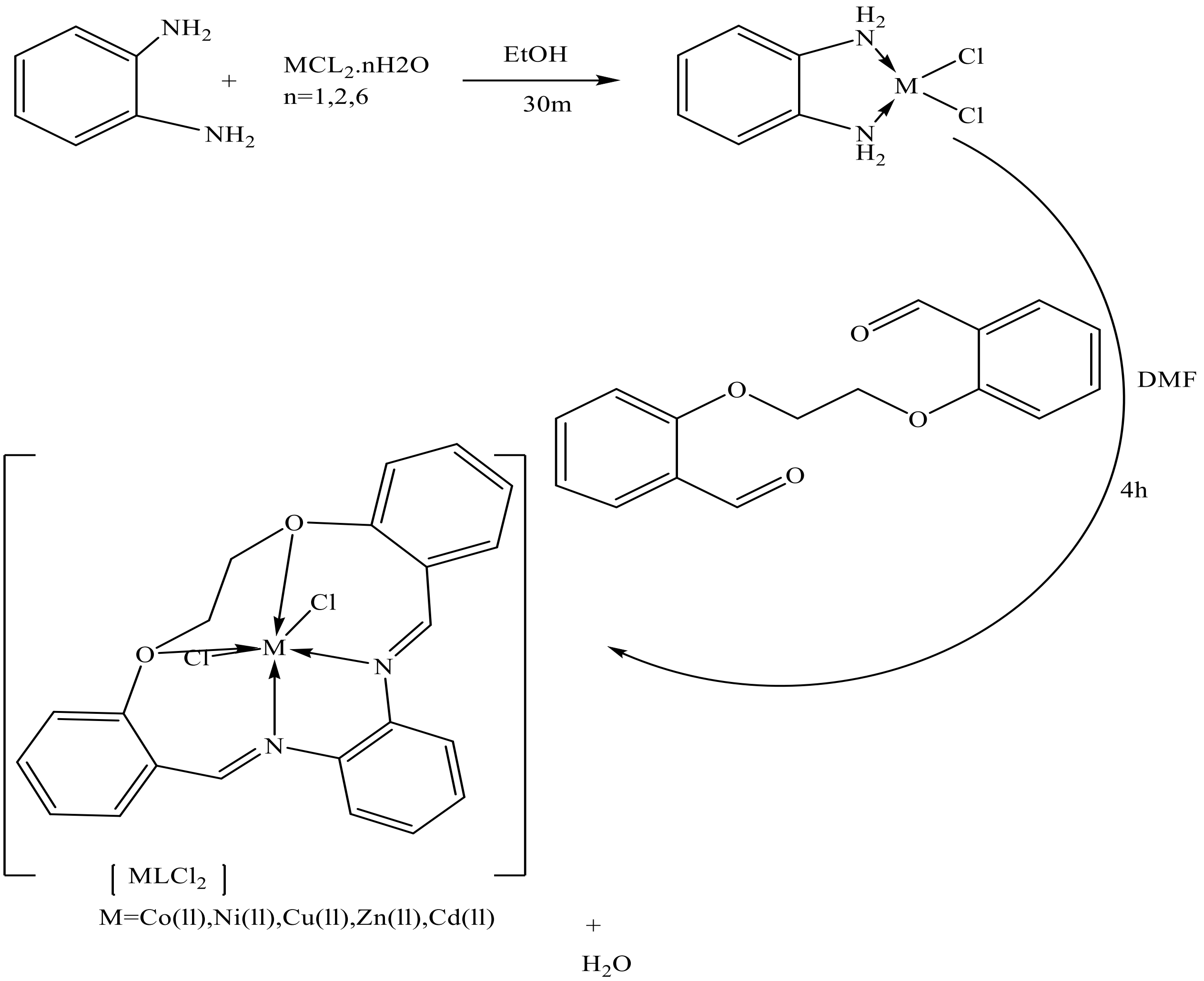

Scheme (2): The Synthesis of the complexes.

Study of Antioxidant Activity Using (DPPH) Method

1. Preparation of Stock Solution of Gallic Acid: (10 mmol L^{-1}) a stock solution of Gallic acid is prepared by dissolving (85 mg) Gallic acid in ethanol and diluting to the mark in (50 ml) volumetric flask and prepared five solutions with different concentrations (0.008, 0.004, 0.002, 0.001 and 0.0005 mmol L^{-1}) were prepared from it.

2. Preparation of DPPH Solution: (45µg ml^{-1}) DPPH solution is prepared by dissolving (4.5 mg) 2,2diphenyl picrylhydrazyl (DPPH) in ethanol and diluting to (100 ml) volumetric flask.

3. Preparation of Stock Solution of compounds prepare different concentrations of four concentrations for each compound, as shown in the table (5).

Results and discussion

The two most crucial aspects of the generated metal complexes are their thermal stability or the makeup of the colored solid. Soluble in DMSO and DMF solvents. For every constructed complex, both the theoretical and the practical data of (C.H.N.) Microanalysis were estimated (Table 1).

No	**Empirical formula**	**M.wt g/mol**	**Yield %**	**Color**	**m.p. °C**	**Microanalysis found, (Calc.)**					
						O	**Metal**	**C**	**H**	**N**	**Cl**
1	[$C_{22}H_{18}N_2O_2$]	344.71	53.24	Dark black	160-164	-------	------	55.68 (55.95)	4.25 (3.81)	6.46 (5.93)	-------
2	[$CoC_{22}H_{18}N_2O_2Cl_2$]	471.82	53.24	black	>300	6.4 (6.7)	12.98 (12.46)	56.68 (55.95)	4.25 (3.81)	5.24 (5.93)	14.76 (15.0)
3	[$NiC_{22}H_{18}N_2O_2Cl_2$]	471.5	65.62	Brown	>300	6..35 (6.7)	13.08 (12.41)	55.12 (55.99)	4.35 (3.81)	6.46 (5.93)	14.82 (15.0)
4	[$CuC_{22}H_{18}N_2O_2Cl_2$]	476.45	75.51	black	218-220	--------	13.85 (13.31)	---------	-------	-------	14.25 (14.95)
5	[$ZnC_{22}H_{18}N_2O_2Cl_2$]	478.31	61.53	Brown	>300	6.26 (6.69)	14.01 (13.65)	54.89 (55.19)	3.08 (3.76)	6.39 (5.83)	14.38 (14.84)
6	[$CdC_{22}H_{18}N_2O_2Cl_2$]	525.31	66.16	Pale brown	>300	-------	21.95 (21.37)	-------	-------	-------	12.98 (13.5)

(Calc)= Calculated

FTIR spectra

After compound (N) reacted with (O-phenylene diamine), compound (L) was created. The characteristic bands of the FTIR spectrum were found to be (3054) cm^{-1} for the aromatic υ (CH), (2924-2876) cm^{-1} for the aliphatic υ (C-H) stretching vibration, (3303-3267) cm^{-1} for the (NH-) groups, (1593) cm^{-1} for the aromatic ring group of the C=C, (1219) cm^{-1} for the ω (C-O) ether group, and (1659) cm^{-1} for the (C=N) groups .[14]. A summary of the distinctive band assignments is provided . The complexes' infrared spectra. That assertion would be supported by the occurrence of a substantial signal that 1659 cm^{-1} that is suggestive of a (C=N) stretch space [15]. The vibrations caused by stretching of aliphatic CH_2 are characterized by strong signals that 2927 & 2872 cm^{-1} [16]. The C=C phenyl group and C-C groups, respectively, are responsible for the bands at 1525 and 1359–1334 cm^{-1}. Additionally, ʋ(C–O), which is located between 1120-1114 cm^{-1}, is the site of the aromatic ring where C–O is bonded. the bands for the ethoxy group about 1280–1200 cm^{-1} ʋ(C–O). It is possible to credit the bands at 762-749 and 582-525 cm^{-1} to (M-N) and (M-O) stretching, respectively [17].

Table (2): FTIR spectral data (wave number ν) cm-^{1}of the ligand L and its complexes.

Compound	**ʋ (C-H) aliph.**	**ʋ (C-H) arom.**	**ʋ (C=C)**	**ʋ (M-O)**	**ʋ (M-N)**	**ʋ (C=N)**	**ʋ(O-C)**
L	2923-2876	3055	1525	-------	-------	1659	1120
[CoL Cl_2]	2939-2872	-----	-------	525	750	1657	1115
[NiLCl_2]	2952-2873	3019	-------	581	748	1604	1118
[CuLCl_2]	---------	--------	1533	580	762	1662	1120
[ZnLCl_2]	--------	3007	1523	539	749	1658	-----
[CdLCl_2]	2949	3014	1610	582	755	1685	1114

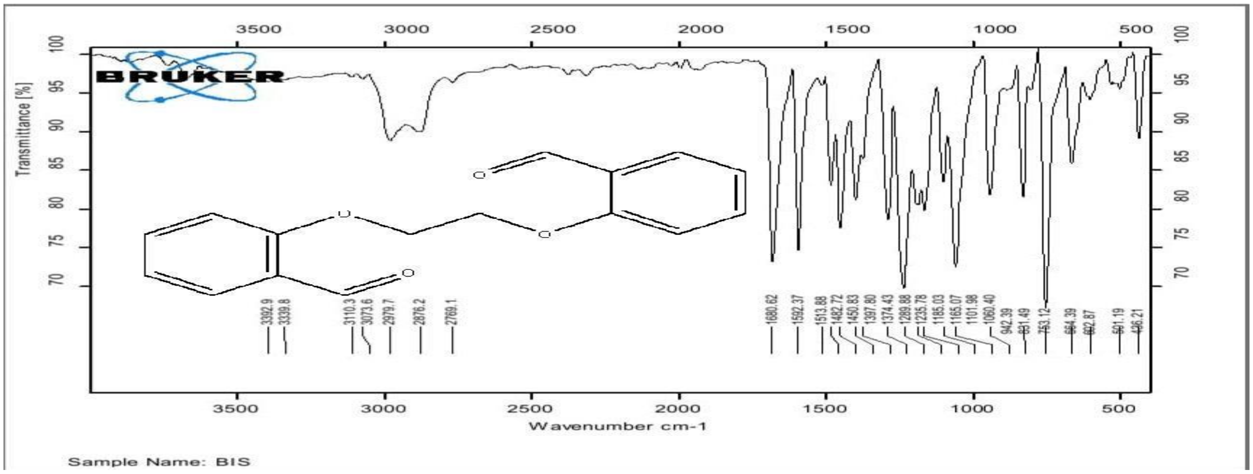

Figure (1): FTIR spectrum of the ligand (N)

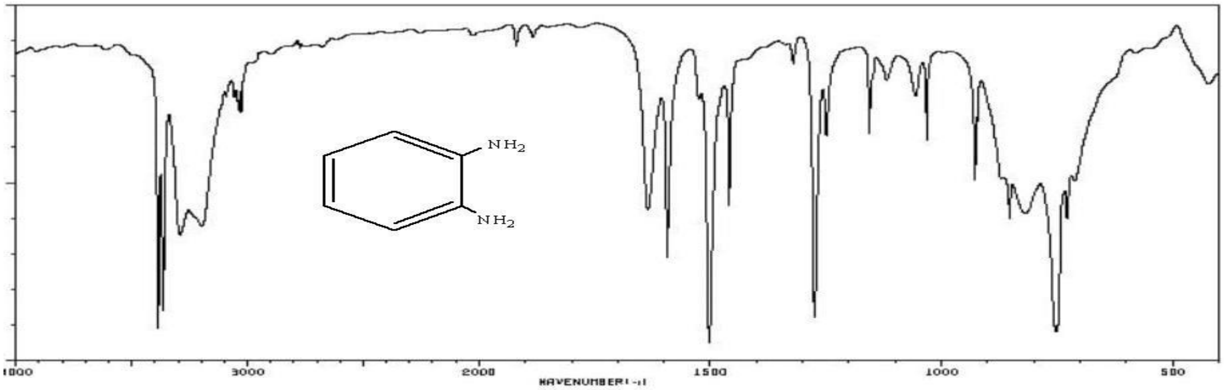

Figure (2): FTIR spectrum of the O-phenlyene diamine

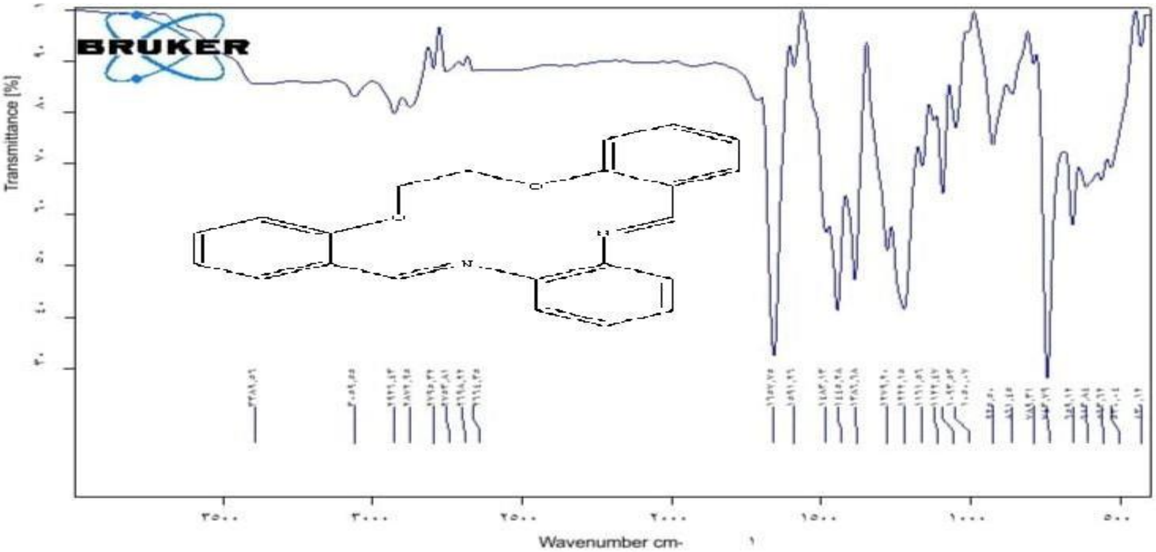

Figure (3): FTIR spectrum of the Ligand L

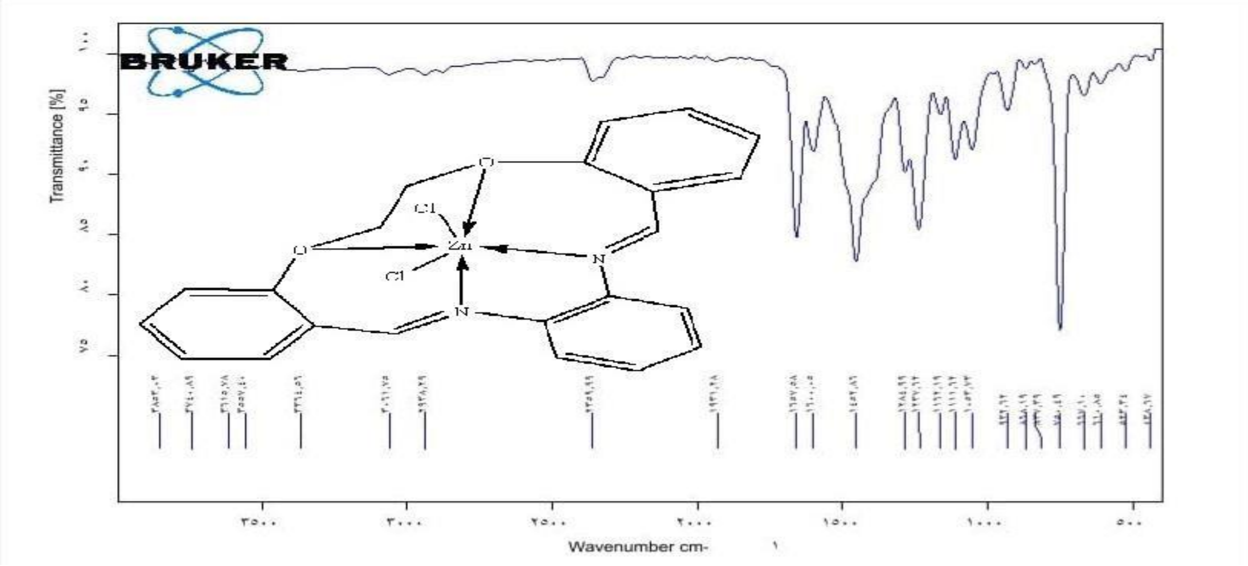

Figure (4): FTIR spectrum of [Zn L Cl_2] complex.

^{1}HNMR Spectra

Figure (5) shows the ^{1}H-NMR spectra of the ligand L. The singlet signal in the spectrum at = 9.0 ppm was attributed to the single proton in the H-C=N group. displays the typical chemical shift (with DMSO-d^6 as the solvent) as follows:. The aromatic portion of the spectrum displayed multiple signals between 8.00 and 7.00 ppm [18]. Four protons are assigned to the multiple chemical shifts at 7.68-7.65 ppm (4H, m, C6,6; 4,4-H). Two protons are represented by a doublet peak at 7.34–7.32 ppm, which can be attributed for (2H, d, C3,3,-H J = 8.2 Hz). At 7.11–7.08 ppm, the triplet peak corresponds to two protons and has been assigned at (2H, t, C5,5~-H }, J = 7.45, 7.50 Hz). At 1.00 ppm, a singlet associated with the ethyl group was found (4H, d,C1,1*). [19]. The spectra showed signals associated with the DMSO-d^6 at roughly 2.50 and 3.33 ppm.

Figure (6) of the ^{13}C-NMR spectrum in DMSO-d^6 solvent displays several signals that are linked to ligand L, which are described as follows: The detection of a signal that δ=195.0 ppm, which is attributed to the atom of carbon C8 for N=C in the group, has revealed the synthesis of the free ligand. The compound's correct resonances were indicated by the spectra. The C=C group resonance associated with C9,9* was observed as a two-signal at δ c = 163.4 ppm. Two signals appeared, indicating as both C= N group are marginally unequal in the solution [20]. This is consistent with Figure 3's FT-IR data, which shows that the two groups are likewise in equivalent non the solid state. A C2.2*-related signal was detected at δ C= 164.5 ppm. Corresponding resonances to C4.4* and C6.6**, $C_{5.5*}$, $C_{7.7*}$, and $C_{3.3*}$ were observed at 158.2, 150.0, 138.5, and 122-121 ppm, respectively, were detected. The two methyl groups, O-C1,1-, were found at

53.00–51.00 ppm and seemed to be equivalent [21]. the chemical shifts at δ - 40.0 ppm that the solvent DMSO is responsible for.

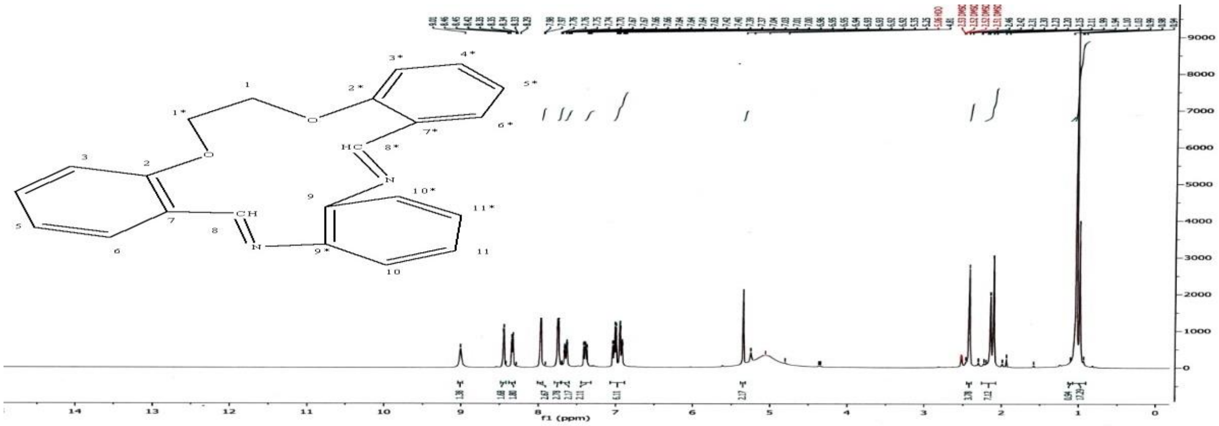

Figure (5) : ^{1}H-NMR spectrum for the ligand L

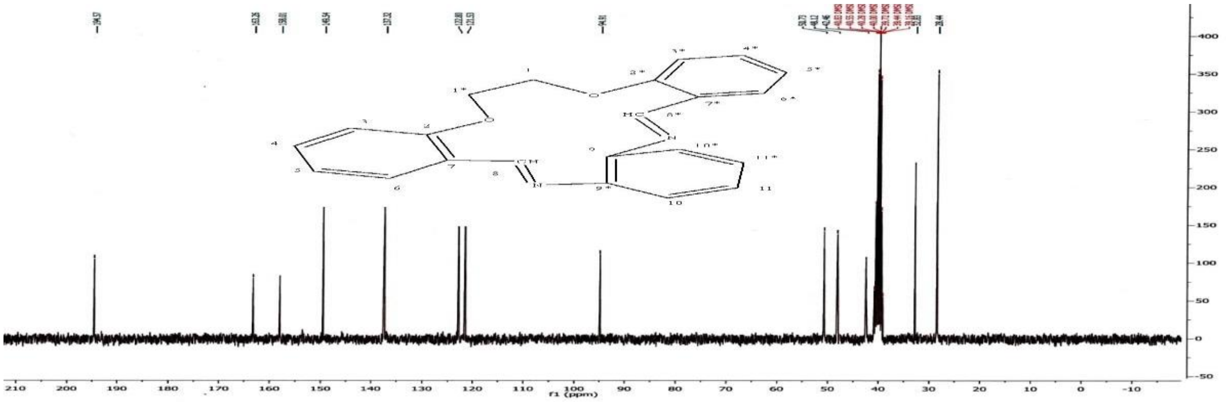

Figure (6) : ^{13}C-NMR for ligand L

The spectrum of mass Figure (7) shows the electrospray (+) masses spectrum of L. The spectrum shows ligand structure-related fragments one after the other. The ligand's parent ion peak is found at m/z = 344, which is equivalent to (M-H(10%)) $C_{22}H_{18}N_2O_2$ required = 342.

Table (3) displays more fragments together with their relative number and fragmentation pattern. A peak at (m/z=475.11) is indicated, and it correlates with the molecule weight of the complex. Theoretical targets include g/mol 476.45 and the occurrence of numerous fissions as a result of fragmentation. The compound. The complexes' mass spectrum is displayed in Figure (8).

Table (3) displays the ratio of abundance and fragmentation pattern of ligand.

Fragment	Mass/charge (m/z)	Relative Abundance
$[M]^+=[C_{22}H_{17}N_2O_2]^+$	344	15%
$[C_{22}H_{20}N_2O]^+$	325.41	40%
$[C_{21}H_{18}N_2O]^+$	309.43	65%
$[C_{14}H_{13}N_2O]^+$	217.31	28.4%
$[C_7H_6NO]^+$	125.44	77%
$[C_6H_5O]^+$	92.74	42%
$[C_7H7]^+$	91.31	100%

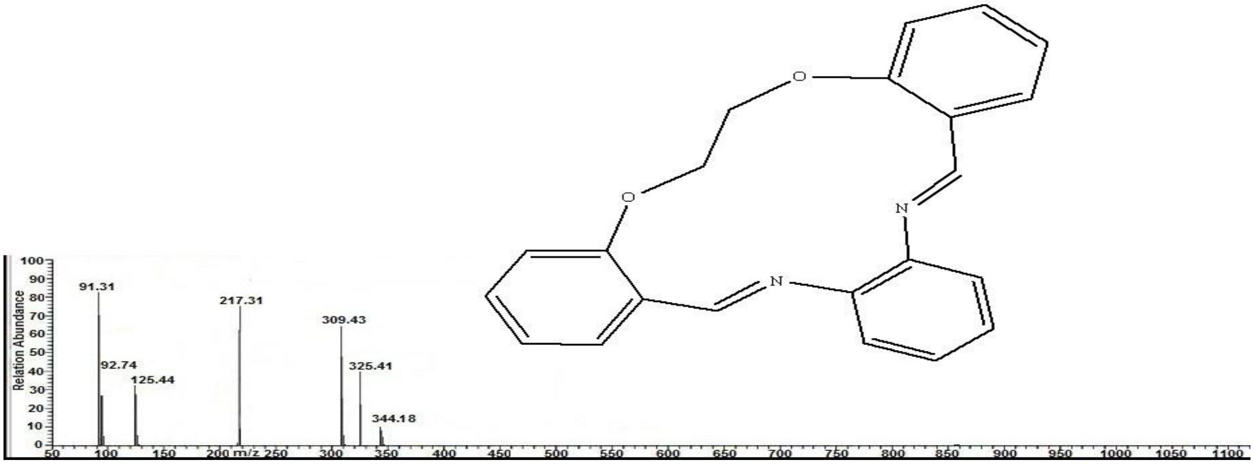

Figure (7) Mass spectrum of free ligand(L)

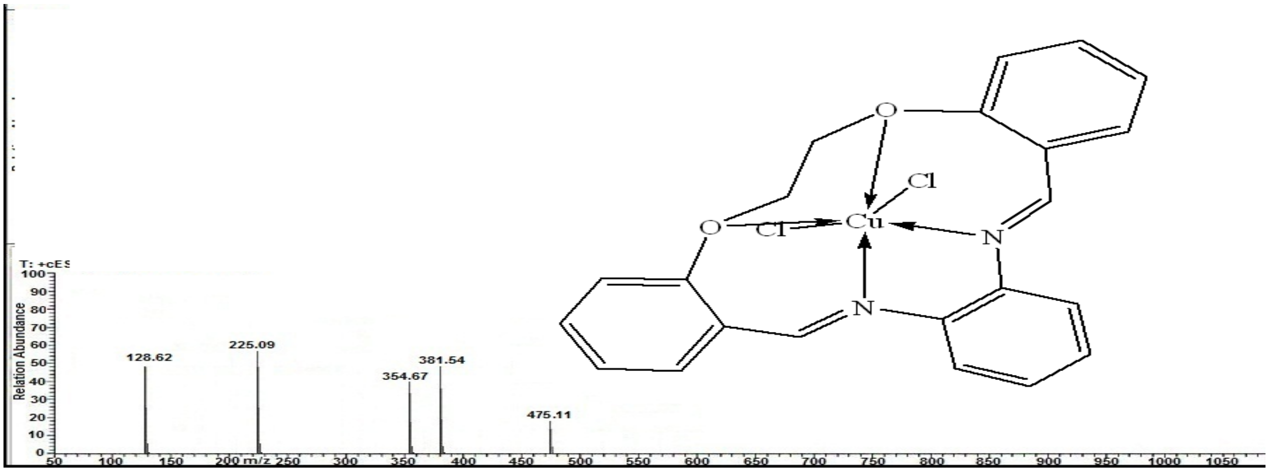

Figure (8) Mass spectrum of the complexes[$CuC_{22}H_{18}N_2O_2Cl_2$

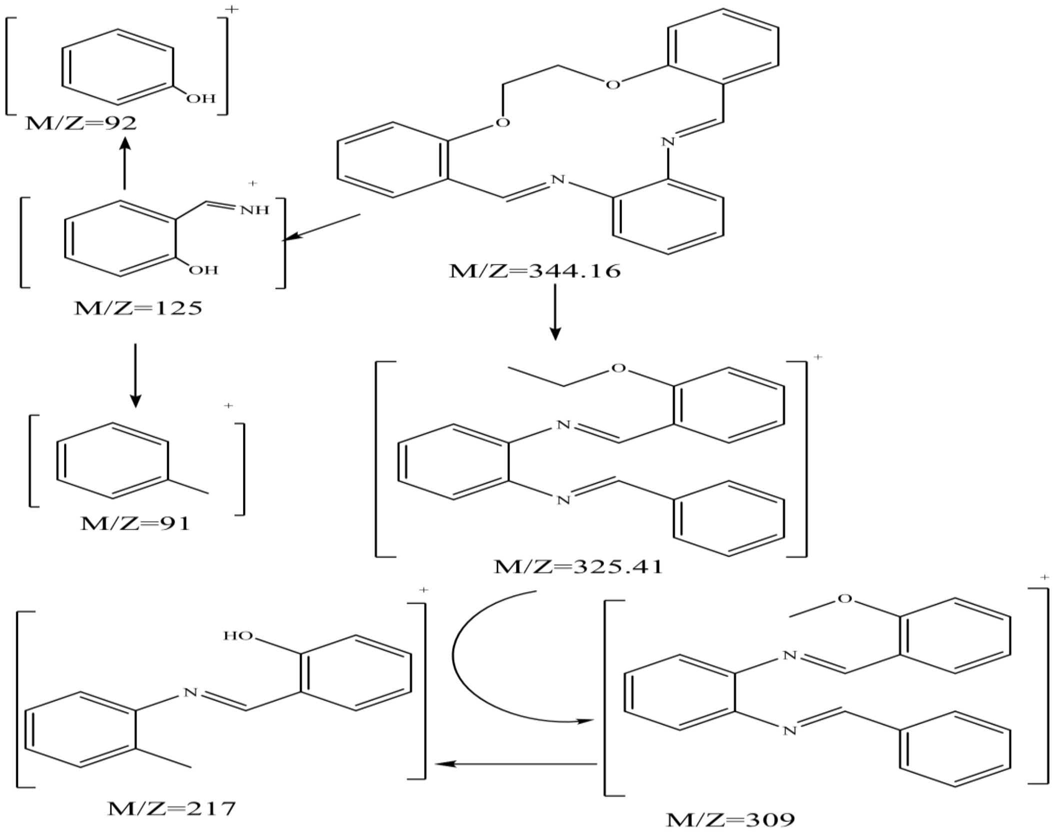

Scheme (3): The fragments of the ligand L .

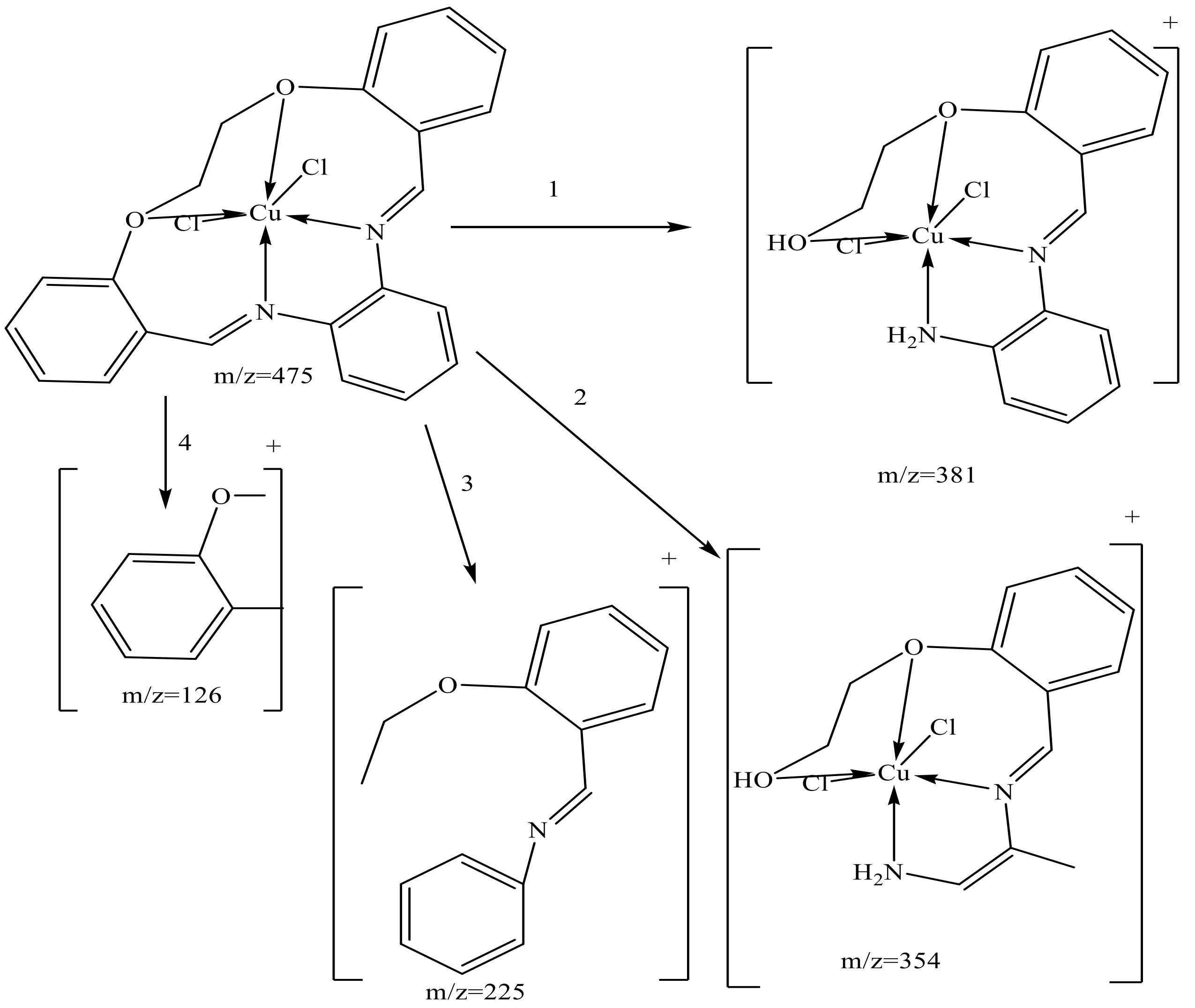

Scheme (4) Fragment of complexes [CuLCl$_2$].

The UV-Vis spectra.

The absorption peaks are visible in Figure (9) UV-Vis spectra of L in DMSO solution, at (282 nm = 35087 cm^{-1}; Ɛ max = 11280 molar^{-1} cm^{-1}) and (given to π→ π* transitions, respectively) [22].

The Co(ll)-complex's electronic spectrum shows three peaks, as seen in Figure (10) The first high intensity peaks are located at (315 nm = 3174 cm^{-1}; Ɛ max = 75000 molar^{-1}.cm^{-1}) and (285 nm = 3508 cm^{-1} ,Ɛ max = 61956 molar^{-1}.cm^{-1}). were allocated to the field of ligands (L.F). An octahedral shape surrounding the Co(ll) central metal ion is confirmed by the peaks, which are seen at (986 nm=1014 cm^{-1} , Ɛ max=9860 molar^{-1}.cm^{-1}) and attributed the d-d electronic types (4T 1 g (F) →4A2 g(F)) transition, respectively [22].

A ligand field (L.F) was ascribed to the two highly intense peak in the Ni (ll)-complex figure's electronic spectra (280nm=3571 cm^{-1}; Ɛ max=25454 molar^{-1}. Cm^{-1}) & (338nm=2958 cm^{-1}; Ɛ max = 13520 molar^{-1}. Cm^{-1}). The visible region is where the peak is located (965nm=1036cm^{-1}; Ɛ max ≈ 9650 molar^{-1}. Cm^{-1}). This peak is attributed to the 3A2g(F) → 3T2g(f) d-d electronic transition type, confirming an octahedral structure around the Ni(ll) ion complex.[23]

The ligand field is ascribed to intense values in the Cu-complex electronic spectrum (282nm=3546 cm^{-1}; max = 11280molar^{-1}.cm^{-1}). Additionally, a charge transfer transition-related peak can be found in the range (405nm=2469 cm^{-1}; Ɛ max = 73636 molar^{-1}. Cm^{-1}). The visible region is where the peak is located (987nm=1013cm^{-1}, Ɛ max = 1977400 molar^{-1}. Cm^{-1}). The d-d transition to the electronic type (2Eg → 2T2g) is attributed to this peak. resolution confirms a warped octahedral configuration surrounding the Cu(ll) ion complex .[22].

The Zn (ll) and Cd(ll) -complexes' electronic spectra are shown in Figure for each case.
For the Zn (ll) and Cd(ll) -complexes, respectively, the ligand field was assigned to peaks in the U.V region at (287 nm=3484 cm^{-1} :Ɛ max= 11480 molar^{-1}.cm^{-1}, 226 nm=4424 cm^{-1}; Ɛ max=46122 molar^{-1}.cm^{-1}) and (294 nm=3401cm^{-1}; Ɛ max=19600 molar^{-1} .cm^{-1}; 313 nm=3194 cm^{-1}; Ɛ max =20866 molar^{-1}.cm^{-1}) respectively. the metals ion of the complexes belongs the d^{10} systems do not show d-d the transition, because filled d orbitals .[24]

Table (4): The UV-Vis spectral data of the ligand L and its complexes .

No	Complexes	Wavenumber		Ɛ max molar^{-1} .cm^{-1}	Assignment	□m (ohm^{-1} .cm^2. mol^{-1})	Ratio	μ$_{eff.}$ B.M
		Nm	cm^{-1}					
1	**L**	282	35087	11280	$\pi\rightarrow\pi^*$			
2	**[Co(L) Cl$_2$]**	285	3508	61956	L.F	13	non-electrolyte	**1.97**
		315	3174	75000	L.F			
		986	1014	9860	$_{4}T_{1}g_{(F)}\rightarrow{}_{4}A_{2}g_{(F)}$			
3	**[Ni(L)Cl$_2$]**	280	3571	25454	L.F	10	non-electrolyte	2.42
		338	2958	13520	L.F			
		665	1036	9650	$_{3}A_{2}g_{(F)}\longrightarrow{}_{3}T_{1}g_{(F)}$			
4	**[Cu(L)Cl$_2$]**	282	3546	11280	L.F	11	non-electrolyte	**2.70**
		405	2469	73636	C.T			
		987	1013	197400	$_{22}T_{2}g\ Eg\longrightarrow$			
5	**[Zn(L)Cl$_2$]**	287	3484	11480	L.F	8	non-electrolyte	Diamagnetic
		226	4424	461122	L.F			
6	**[Cd(L)Cl$_2$]**	2294	3401	19600	L.F	16	non-electrolyte	Diamagnetic
		313	3194	20866	L.F			

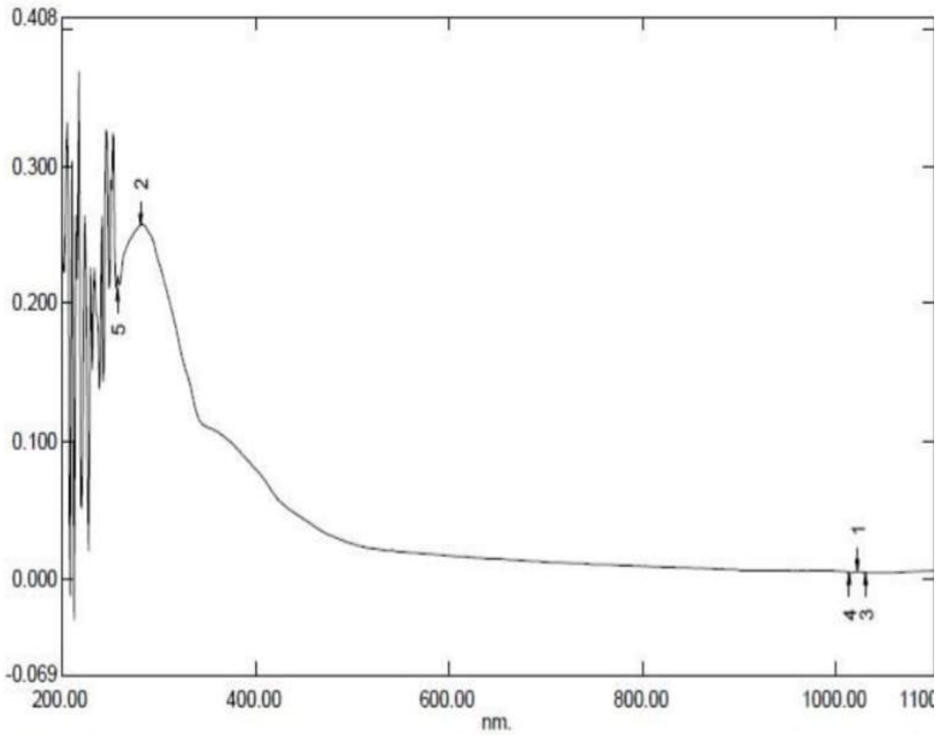

Figure (9) The UV-Vis spectrum of L

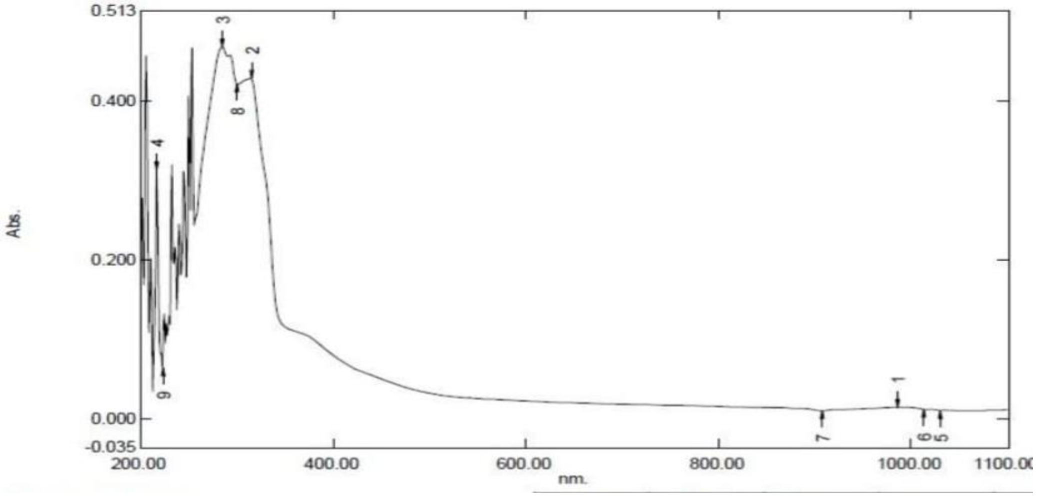

Figure (10) The UV-Vis spectrum of[$CoLCl_2$]

The antioxidant activity of the compounds was determined by free radical trapping test using DPPH. When DPPH reacts with compounds, it changes color from purple to yellow at a wavelength (517 mm) using an ultraviolet visible device.

The free radical scavenging activity of gallic acid was compared with compounds using the free radical scavenging agent DPPH. Free radicals were captured by antioxidants after reduction, and were measured by the decrease in absorbance at a wavelength of 517 mm. Gallic acid showed greater antioxidant activity after 60 minutes. The compounds are ranked according to their ability to suppress free radicals, which is based on IC50 values. The lower the value, the greater its ability to suppress free radicals. The compounds were arranged as follows :Co L> Gallic acid >L > Cu L. According to its ability to catch space [25,26] .

compound	Concentration	PI%	RSA%	IC_{50} mg/mL
Gallic acid	0.008	20.73	79.27	0.004
	0.004	47.69	52.31	
	0.002	62.35	37.65	
	0.001	70.16	29.84	
	0.0005	76.36	27.64	
L	0.008	34.61	65.39	0.0085
	0.004	47.42	52.58	
	0.002	54.36	45.64	
	0.001	64.37	35.63	
Cu L Cl_2	0.008	45.36	54.64	0.022
	0.004	53.33	46.67	
	0.002	58.28	41.72	
	0.001	67.16	32.84	
Co L Cl_2	0.008	56.03	43.97	0.0018
	0.004	60.16	39.84	
	0.002	67.34	32.66	
	0.001	70.12	29.88	

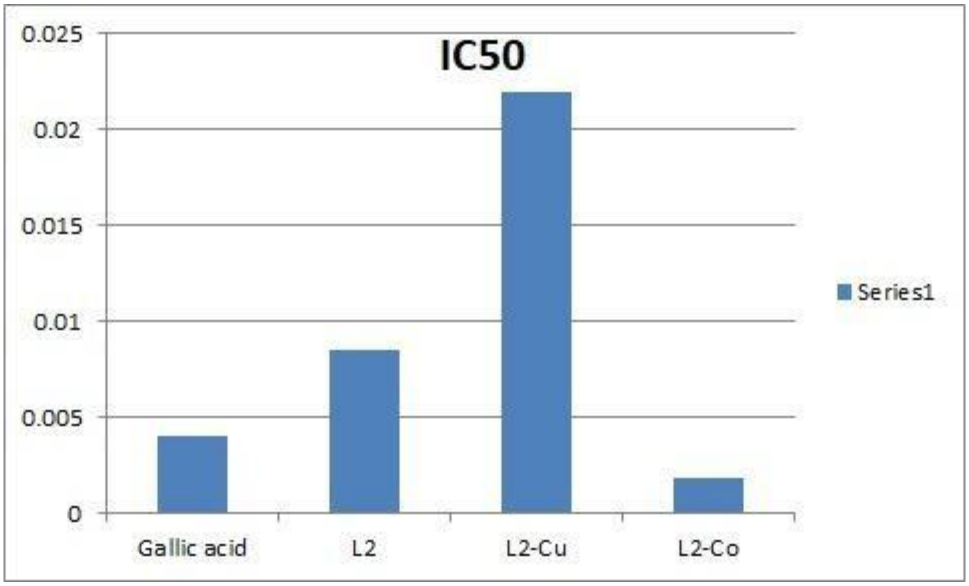

Conclusion

A ligand (L) or its novel metal complexes are synthesized and characterized and reported. The two C=N & two ether-oxygen donation atoms that make up the tradentate ligand were produced in two steps. The formation of monomeric complexes was the outcome of the ligand's interaction with metal ions of (Co(ll), Ni(ll) , Cu(ll) ,Zn(ll)) and Cd(ll) in a (1L: 0.5M)mole ratio. Physicochemical approaches were utilized to verify the chemistry of compounds and their overall bonding behavior. The separation of the octahedral coordinated complex of the general formula & six-coordinate monomeric complex of the general [MLC12] (when M= Co (ll) ,Ni (ll) and Cu(ll)) was validated by the characterization results.

REFERENCES :

[1] Vögtle, F., & Weber, E. (Eds.). (2012). *Host Guest Complex Chemistry Macrocycles: Synthesis, Structures, Applications*. Springer Science & Business Media.

[2] Rosu, T., Pahontu, E., Ilies, D. C., Georgescu, R., Mocanu, M., Leabu, M., ... & Gulea, A. (2012). Synthesis and characterization of some new complexes of Cu (II), Ni (II) and V (IV) with Schiff base derived from indole-3-carboxaldehyde. Biological activity on prokaryotes and eukaryotes. *European journal of medicinal chemistry*, *53*, 380-389.

[3] Firdaus, F., Fatma, K., Azam, M., Khan, S. N., Khan, A. U., & Shakir, M. (2008). Template synthesis and physicochemical studies of 14-membered hexaazmacrocyclic complexes with Co (II), Ni (II), Cu (II) and Zn (II): a comparative spectroscopic approach on DNA binding with Cu (II) and Ni (II) complexes. *Transition Metal Chemistry*, *33*, 467-473.

[4] Shakir, M., Khanam, S., Azam, M., Aatif, M., & Firdaus, F. (2011). Template synthesis and spectroscopic characterization of 16-membered [N4] Schiff-base macrocyclic complexes of Co (II), Ni (II), Cu (II), and Zn (II): in vitro DNA-binding studies. *Journal of Coordination Chemistry*, *64*(18), 3158-3168.

[5] Abdel-Rahman, L. H., Abu-Dief, A. M., Adam, M. S. S., & Hamdan, S. K. (2016). Some new nano-sized mononuclear Cu (II) Schiff base complexes: design, characterization, molecular

modeling and catalytic potentials in benzyl alcohol oxidation. *Catalysis Letters*, *146*, 1373-1396.

[6] Rahman, L. H. A., Abu-Dief, A. M., El-Khatib, R. M., & Abdel-Fatah, S. M. (2018). Sonochemical Synthesis, Spectroscopic Characterization, 3D Molecular Modeling, DNA Binding and Antimicrobial Evaluation of some Transition Metal Complexes Based on Bi-dentate NO Donor Imine Ligand. *Int. J. Nano. Chem*, *4*(1), 1-17.

[7] Elshafaie, A., Abdel-Rahman, L. H., Abu-Dief, A. M., Hamdan, S. K., Ahmed, A. M., & Ibrahim, E. M. M. (2018). Electric, thermoelectric and magnetic properties of Nickel (II) Imine Nanocomplexes. *Nano*, *13*(07), 1850074.

[8] Abou-Hussein, A. A., & Linert, W. (2015). Synthesis, spectroscopic studies and inhibitory activity against bactria and fungi of acyclic and macrocyclic transition metal complexes containing a triamine coumarine Schiff base ligand. *Spectrochimica Acta Part A: Molecular and Biomolecular Spectroscopy*, *141*, 223-232.

[9] Shreaz, S., Shiekh, R. A., Raja, V., Wani, W. A., & Behbehani, J. M. (2016). Impaired ergosterol biosynthesis mediated fungicidal activity of Co (II) complex with ligand derived from cinnamaldehyde. *Chemico-biological interactions*, *247*, 64-74..

[10] El-Boraey, H. A. (2012). Coordination behavior of tetraaza [N4] ligand towards Co (II), Ni (II), Cu (II), Cu (I) and Pd (II) complexes: synthesis, spectroscopic characterization and anticancer activity. *Spectrochimica Acta Part A: Molecular and Biomolecular Spectroscopy*, *97*, 255-262.

[11] Andrew, F. P., & Ajibade, P. A. (2018). Synthesis, characterization and anticancer studies of bis-(N-methyl-1-phenyldithiocarbamato) Cu (II), Zn (II), and Pt (II) complexes: Single crystal X-ray structure of the copper complex. *Journal of Coordination Chemistry*, *71*(16-18), 2776-2786.

[12] Akkurt, M., Mohamed, S. K., Horton, P. N., Abdel-Raheem, E. M., & Albayati, M. R. (2013). 2, 2′-[Ethane-1, 2-diylbis (oxy)] dibenzaldehyde. *Acta Crystallographica Section E: Structure Reports Online*, *69*(8), o1260-o1260.

[13] Fahmi, N., Upadhyay, M., Sharma, N., & Belwal, S. (2020). Synthesis, characterization and biochemical behaviour of macrocyclic complexes of Zn (II) and Co (II) metals. *Journal of Chemical Research*, *44*(5-6), 336-342.

[14] Jassim, I. K., Mohammed, I. Y., & Salman, S. (2020). Synthesis of anti-corrosion polymers from thiadiazole. In *IOP Conference Series: Materials Science and Engineering* (Vol. 736, No. 4, p. 042042). IOP Publishing.

[15] Shalabi, K., El-Gammal, O. A., & Abdallah, Y. M. (2021). Adsorption and inhibition effect of tetraaza-tetradentate macrocycle ligand and its Ni (II), Cu (II) complexes on the corrosion of Cu10Ni alloy in 3.5% NaCl solutions. *Colloids and Surfaces A: Physicochemical and Engineering Aspects*, *609*, 125653.

[16] K B Benzon , Hema Tresa Varghese , C Yohannan Panicker , Kiran Pradhan , Bipransh Kumar Tiwary , Ashis Kumar Nanda , C Van Alsenoy (2015)"Spectroscopic investigation (FT-IR and FT-Raman), vibrational assignments, HOMO–LUMO, NBO, MEP analysis and molecular docking study of 2-(4hydroxyphenyl)-4, 5-dimethyl-1H-imidazole 3-oxide," *Spectrochim. Acta Part A Mol. Biomol. Spectrosc.*, vol. 146, pp. 307–322

[17] Mihsen, H. H., Abass, S. K., Abass, A. K., Hussain, K. A., & Abbas, Z. F. (2018). Template Synthesis of Sn (II), Sn (IV) and Co (II) complexes via 3-Aminopropyltriethoxysilane and Salicylaldehyde and Evaluate their Antibacterial Sensitivity. *Asian J. Chem*, *30*, 2277-2280.

[18] Chandini, K. M., Al-Ostoot, F. H., Shehata, E. E., Elamin, N. Y., Ferjani, H., Sridhar, M. A., & Lokanath, N. K. (2021). Synthesis, crystal structure, Hirshfeld surface analysis, DFT calculations, 3D energy frameworks studies of Schiff base derivative 2, 2′-((1Z, 1′ Z)-(1, 2-phenylene bis (azanylylidene)) bis (methanylylidene)) diphenol. *Journal of Molecular Structure*, *1244*, 130910.

[19] BAOUAB, M. H. V., Fra, S. B. H., Chaabene, M., Agren, S., Lahcini, M., & Chaâbane, R. B. (2022). High incorporation of magnetite nanoparticles inside tetraaza macrocyclic Schiff base cavity: Spectroscopic characterization and modeling by DFT calculation.

[20] Yerrasani, R., Karunakar, M., Dubey, R., Singh, A. K., Nandi, R., Singh, R. K., & Rao, T. R. (2016). Synthesis, characterization and photophysical studies of rare earth metal complexes with a mesogenic Schiff-base. *Journal of Molecular Liquids*, *216*, 510-515.

[21] Manesh, A. A., & Zebarjadian, M. H. (2020). Synthesis of three new branched octadentate (N8) Schiff Base and competitive Lithium-7 NMR study of the stoichiometry and stability constant of Mn2+, Zn2+ and Cd2+ complexes in acetonitrile–[(BMIM)(PF6)] mixture. *Journal of Molecular Structure*, *1199*, 126965.

[22] Yadav, M., Sharma, S., & Devi, J. (2021). Designing, spectroscopic characterization, biological screening and antioxidant activity of mononuclear transition metal complexes of bidentate Schiff base hydrazones. *Journal of Chemical Sciences*, *133*, 1-22.

[23] Al-Hamdani, A. A. S., BALKHI, A., Falah, A., & Shaker, S. A. (2015). New azo-Schiff Base derived with Ni (II), Co (II), Cu (II), Pd (II) and Pt (II) complexes: preparation, spectroscopic investigation, structural studies and biological activity. *Journal of the Chilean Chemical Society*, *60*(1), 2774-2785.

[24] Al-Adilee, K., & Kyhoiesh, H. A. (2017). Preparation and identification of some metal complexes with new heterocyclic azo dye ligand 2-[2−-(1-Hydroxy-4-Chloro phenyl) azo]-imidazole and their spectral and thermal studies. *Journal of Molecular Structure*, *1137*, 160-178.

[25] Vhanale, B., Kadam, D., & Shinde, A. (2022). Synthesis, spectral studies, antioxidant and antibacterial evaluation of aromatic nitro and halogenated tetradentate Schiff bases. *Heliyon*, *8*(6).

[26] Abdulridha, M. Q., Al-Hamdani, A. A. S., & Hussein, I. A. (2023). Synthesis, Characterization and Antioxidant Activity of New Azo Ligand and Some Metal Complexes of Tryptamine Derivatives. *Baghdad Science Journal*, *20*(3 (Suppl.)), 1046-1046.